

Model Predictive Control Design for Unlocking the Energy Flexibility of Heat Pump and Thermal Energy Storage Systems

Weihong Tang¹, Yun Li¹, Shalika Walker², Tamas Keviczky¹

Abstract—Heat pump and thermal energy storage (HPTES) systems, which are widely utilized in modern buildings for providing domestic hot water, contribute to a large share of household electricity consumption. With the increasing integration of renewable energy sources (RES) into modern power grids, demand-side management (DSM) becomes crucial for balancing power generation and consumption by adjusting end users' power consumption. This paper explores an energy flexible Model Predictive Control (MPC) design for a class of HPTES systems to facilitate demand-side management. The proposed DSM strategy comprises two key components: i) *flexibility assessment*, and ii) *flexibility exploitation*. Firstly, for *flexibility assessment*, a tailored MPC formulation, supplemented by a set of auxiliary linear constraints, is developed to quantitatively assess the flexibility potential inherent in HPTES systems. Subsequently, in *flexibility exploitation*, the energy flexibility is effectively harnessed in response to feasible demand response (DR) requests, which can be formulated as a standard mixed-integer MPC problem. Numerical experiments, based on a real-world HPTES installation, are conducted to demonstrate the efficacy of the proposed design.

I. INTRODUCTION

Climate change has emerged as a pressing global concern, and prompts global actions. To achieve carbon neutrality and sustainable energy usage, the European Union has set an ambitious goal to increase the share of renewable energy sources (RES), such as solar energy and wind energy, to at least 27% by 2030 [1]. However, it is well-known that due to the intermittency and volatility of RES, growing reliance on the electricity generation from RES can introduce significant challenges in balancing supply and demand in the power grid, and hence lead to congestion. As a response, the concept of demand-side management (DSM) is proposed, which entails adjusting the energy consumption of end users according to the needs of the power grid, to balance the real-time power generation and consumption [2], [3].

As an energy efficient and low-carbon thermal generation option, heat pumps (HP) are widely adopted in Europe to provide thermal energy in buildings, such as floor heating and domestic hot water usage, and the number of installations are on a sharp rise. It is estimated that by 2027, 10 million additional heat pumps will be installed in the EU [4]. A typical utilization of HPs is the combination of HP and

thermal storage system, which we refer to as HPTES in this paper. With the support of TES, the thermal energy generated by HPs can be stored, which largely increases the flexibility of electricity consumption of HPs [5]. Considering the large amount of energy consumption of HPs in buildings and the energy flexibility emanating from HPTES systems, it is of interest to investigate potential improvements or replacement of the existing rule-based control schemes in HPTES systems for achieving DSM. As an advanced control technique, model predictive control (MPC) is regarded as a promising and effective control scheme to be widely implemented in future building management systems (BMS) due to its versatility in coping with system constraints, economic considerations, as well as the alignment of predicted energy consumption and availability. In [6]–[9] and references therein, MPC-based operation schemes are designed for HPTES systems.

While MPC-based schemes for economic operation of HPTES have been extensively studied in literature and are shown to be effective, when considering DSM in the form of demand response (DR) requests, there is room for further improvement and alternative control schemes. The existing works about DSM of HPTES follow the so-called incentive-based or price-based programs [10], [11]. As pointed out in [12], while such schemes are relatively easy to implement, these programs fall short of full exploitation of energy flexibility and might fail to achieve the expected energy reduction from the power grid. In order to better utilize the energy flexibility of buildings and meet the demands of the power grid, a two-step DSM framework is proposed in [12]. This scheme entails assessing the energy flexibility potential of the system, and a bidirectional communication between BMS and the power grid. Also, this two-step DSM framework fits in the S2 standard that is developed by the European Commission for exploiting energy flexibility in built environment [13].

In this paper, we will design an MPC-based DSM scheme based on the framework proposed in [12] and investigate an energy flexible MPC design for a class of HPTES systems to achieve demand-side management. A general control-oriented model for the HPTES system is introduced. Based on this model, a unified MPC framework for quantitatively assessing the energy flexibility potential of the HPTES system and exploiting the flexibility via DR requests are designed. The proposed flexibility assessment approach only entails considering extra linear constraints within a typical economic MPC problem. With the proposed approach, the energy flexibility emanated from the thermal storage tanks is utilized to solve grid congestion problems without violating

¹W. Tang, Y. Li and T. Keviczky are with the Delft Center for Systems and Control, Delft University of Technology, Delft, the Netherlands. ttonytany@gmail.com; y.li-39@tudelft.nl; T.Keviczky@tudelft.nl

²S. Walker is with the Kropman BV, the Netherlands. shalika.walker@kropman.nl

This work was supported by the Brains4Buildings project under the Dutch grant programme for Mission-Driven Research, Development and Innovation (MOOI).

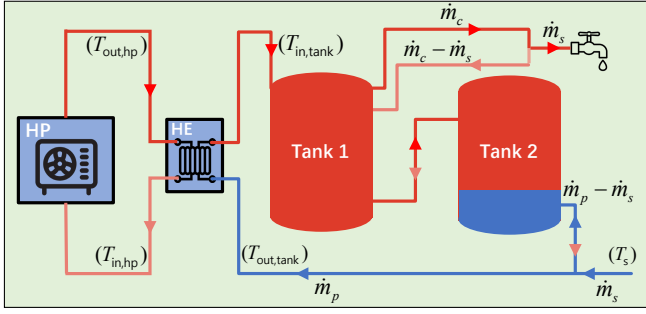


Fig. 1: Diagram of the considered general HPTES system.

system constraints.

The remaining parts of this paper are organized as follows. Section II describes a control-oriented model for the HPTES system. Section III provides a unified MPC design framework for assessing and exploiting the energy flexibility of the HPTES system. Simulation results are presented in Section IV, followed by Conclusions in Section V.

II. HPTES SYSTEM MODELLING AND PROBLEM FORMULATION

In this section, a general control-oriented model of the HPTES system and the corresponding physical constraints are introduced. The HPTES system considered in our work is composed of three main components: a heat pump, a heat exchanger (HE), and two thermal storage tanks. The configuration of the HPTES system that will be investigated is shown in Fig. 1, where blue lines represent cold water flows, red lines represent hot water flows, and arrows represent the flow directions. The mass flow rates and temperature of corresponding pipelines that are used in developing the HPTES model are also indicated. This configuration is based on a typical real HPTES system installation located in an office building in the Netherlands.

Hot water from the top of Tank 1 is circulated at a mass flow rate \dot{m}_c going through connected taps to meet hot water usage demands. The real-time hot water usage is \dot{m}_s , whose future values are assumed to be predictable with sufficient accuracy from historical data. When hot water is consumed, the same amount of cold water \dot{m}_s is supplied to the bottom of Tank 2 at the same time so that the total amount of water in the HPTES system is always constant. If the HP is off, the cold water will be directly injected into the bottom of Tank 2; otherwise, the water from the bottom of Tank 2 with mass flow rate \dot{m}_p will be heated by HP then pumped into the top of Tank 1. The corresponding mass flow rates of the water circulations are indicated in Fig. 1.

In the following, we will provide a general control-oriented model of the above HPTES system, which will be used for our MPC design in Section III.

A. Heat Pump Model

Heat pumps are used for providing thermal energy in the HPTES system. To model the relationship between the electricity consumption and thermal energy generation of HP,

the concept of coefficient of performance (COP) is used. The COP is defined as the ratio of heat output to work input, which can be expressed as

$$\text{COP} = \frac{Q_{\text{hp}}}{P_{\text{hp}}}, \quad (1)$$

where Q_{hp} denotes the heat output of the heat pump and P_{hp} its power input.

It is assumed in our design that the HP only operates in two modes: on and off. Hence, it follows from (1), that the thermal energy generated by HP can be denoted as

$$Q_{\text{hp}} = \text{COP} \cdot P_r \cdot u, \quad (2)$$

where P_r is the rated power of the heat pump, and $u \in \mathbb{B}$ is the on/off binary control signal.

In order to balance approximation accuracy and computational burden of the resulting MPC problem, the following bilinear COP model is adopted:

$$\text{COP} = a_1 + a_2 \cdot T_{\text{in,hp}} + a_3 \cdot T_{\text{amb}} + a_4 \cdot T_{\text{in,hp}} \cdot T_{\text{amb}}, \quad (3)$$

where $T_{\text{in,hp}}$ is the inlet water temperature of HP, T_{amb} is the ambient air temperature of HP, and (a_1, a_2, a_3, a_4) are parameters to be identified.

B. Thermal Energy Storage Model

The thermal energy generated by HP is used to heat the water in the connected water tanks. For modeling the water tanks, the stratified tank model is adopted to balance modeling accuracy and computational burden [14]. In the stratified water tank model, a single water tank is divided into several connected layers, or called nodes. Each layer is assumed to function as an individual node with uniform temperature distribution. The general thermal behavior of each layer is depicted in Fig. 2, where the thermal exchange of each node is composed by the following parts:

- $\dot{Q}_{\text{wall},j}$: the heat loss from layer j to the tank wall.
- $\dot{Q}_{j+1,j}$ and $\dot{Q}_{j-1,j}$: thermal conduction between layer j and its adjacent layers $j+1$ and $j-1$.
- \dot{Q}_{conv} : heat exchange due to water flows \dot{m}_t in/out of j -th layer from/to adjacent layers.

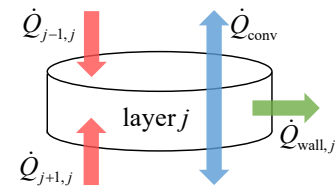


Fig. 2: Heat flow diagram of a single layer of TES.

Then, the thermal dynamics of each thermal node can be

written as

$$m_j c_p \frac{dT_j}{dt} = -\dot{Q}_{\text{wall},j} + \dot{Q}_{j+1,j} + \dot{Q}_{j-1,j} + \dot{Q}_{\text{conv}}, \quad (4a)$$

$$\dot{Q}_{\text{conv}} = \begin{cases} \dot{m}_t c_p (T_{j-1} - T_j), & \dot{m}_t \text{ flows from } j-1 \text{ to } j \\ \dot{m}_t c_p (T_{j+1} - T_j), & \dot{m}_t \text{ flows from } j+1 \text{ to } j \end{cases} \quad (4b)$$

$$\dot{Q}_{j+1,j} = R_{j,j+1} (T_{j+1} - T_j), \quad (4c)$$

$$\dot{Q}_{j-1,j} = R_{j-1,j} (T_{j-1} - T_j), \quad (4d)$$

$$\dot{Q}_{\text{wall},j} = R_w (T_j - T_{\text{amb}}), \quad (4e)$$

where m_j is the mass of the j -th node, c_p is the specific heat capacity of water, \dot{m}_t is the water mass flow rate between adjacent tank layers, $R_{j,j+1}$ and R_w are thermal resistances between the j -th layer and the $(j+1)$ -st layer and the tank wall, respectively.

Equation (4) describes the general thermal behaviour of a water layer. For layers with hot water extraction and cold water supplement, their thermal dynamics need extra modification. For the top layer of Tank 1, it does not have an upper layer so the thermal conduction $\dot{Q}_{j-1,j} = 0$, and the heat convection $\dot{Q}_{\text{conv}} = \dot{m}_t c_p (T_{j-1} - T_j)$ should be computed with T_{j-1} as the temperature of the inlet water injected into Tank 1. The same analysis is also applicable to the bottom layer of Tank 2, where no lower layer exists. In addition, in our system, since the water circulation direction will change with the operation of HP, namely u , the mass flow rate of convection, \dot{m}_t , is a function of HP control signal u and the mass flow rate of hot water consumption \dot{m}_s .

The thermal dynamics in (4) is able of capturing the thermal behaviour of a general thermal storage system and can be easily adapted to other water tank configurations with minor modification. Also, this model is sufficiently simple to be incorporated into MPC design as a prediction model.

C. System Constraints

For safe operation and demand requirements satisfaction, the HPTES system is subject to several physical constraints. In this subsection, we describe the system constraints that the proposed control scheme has to satisfy.

Firstly, to provide qualified hot water and ensuring safe operation, the water temperature of the HPTES system has to be within an admissible range, which is denoted as

$$x^l \leq x \leq x^u, \quad (5)$$

where x denotes the temperature vector of different water layers and pipelines, x^l and x^u are the corresponding temperature lower bound and upper bound, respectively.

Secondly, frequent on-off switches of HP is unfavourable since it can cause excessive wear and tear and reduce the HP lifetime. Consequently, the proposed MPC scheme should prevent frequently switching the HP. For this purpose, the following constraint is added:

$$\sum_{k=1}^m (u_{t-k+1} - u_{t-k})^2 \leq N_{\text{ctrl}}, \quad (6)$$

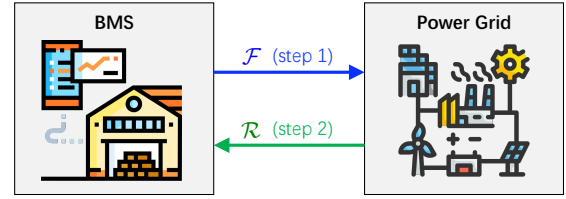


Fig. 3: Diagram of the two-step DSM scheme.

where N_{ctrl} is the maximal number of switches that is allowed during m time steps, and u_{t-k} denotes the control input k time steps in the past compared to the current time instant t . Because $u_t \in \mathbb{B}$, the LHS of (6) computes the number of switches during the most recent m time steps. For instance, setting $m = 8$ and $N_{\text{ctrl}} = 1$ implies that, within an 8-step time window, only one switch is allowed.

Remark 1: The HPTES configuration and the corresponding control-oriented models and system constraints described in this section are general enough to cover a wide range of possible HPTES systems. Also, the control-oriented models can be flexibly adjusted while still keeping a similar model structure even if other alternative configurations are adopted. For example, the position of hot water extraction, which is at the top of Tank 1 in our case, and the position of cold water supplement, which is at the bottom of Tank 2 in our case, can be placed in other positions. Consequently, our MPC-based control design scheme in Section III will also be applicable to these alternative configurations with only minor modifications.

III. ENERGY FLEXIBLE MPC DESIGN FOR DEMAND-SIDE MANAGEMENT

In this section, an MPC strategy is designed for the HPTES system by following the two-step DSM framework shown in Fig. 3. The DSM scheme consists of two steps: flexibility assessment and flexibility exploitation.

As pointed out in [10]–[12], most of the DSM strategies follow either price-based or incentive-based programs, which are both one-step approaches and fail to fully exploit the energy flexibility of the system. With this two-step DSM framework, at *step 1*, the flexibility potential of the HPTES system is assessed by BMS and the flexibility information \mathcal{F} is sent to the grid operator. Then, at *step 2*, the grid operator generates a feasible DR request \mathcal{R} to the BMS to activate the energy flexibility. In contrast to the existing price-based or incentive-based programs, this two-step DSM approach guarantees that the expected DR requests from the power grid will be achieved. This is achieved by quantitatively assessing the flexibility potential of the system before exploitation, and generating feasible DR requests. This property is beneficial in efficiently coordinating different DR service providers and conducting DSM.

A. Flexibility Assessment

The first question to answer for the two-step DSM scheme is how to assess the energy flexibility potential of the HPTES system that is performed in step 1. It has been proposed that

there are three basic factors in determining energy flexibility: magnitude, time duration, and cost [15], [16]. Consequently, we will quantitatively describe the energy flexibility of the HPTES system via these factors.

Since we focus on solving the grid congestion problem, which is currently a challenging issue in the Dutch electricity market, the exploitation of flexibility refers to reducing the electricity consumption of HP. For our considered HPTES system, the control input of HP only has two modes: on and off. Consequently, the capacity of flexibility is proportional to the time duration that HP can remain off. Accordingly, in our work, the goal of flexibility assessment is to determine the optimal flexibility duration to maximize the benefits of providing DR services, i.e., the period during which HP is off without violating system constraints.

To conduct flexibility assessment, we introduce two sets of auxiliary decision variables $\mathcal{S}_{\mathcal{T}} := \{s_t, t \in \mathcal{T}\}$ and $\mathcal{Z}_{\mathcal{T}} := \{z_t, t \in \mathcal{T}\}$, where $s_t \in \mathbb{B}$ and $z_t \in \mathbb{B}$ are binary variables, and $\mathcal{T} := \{t_{f_1}, \dots, t_{f_n}\}$ is the set of time indices during which the flexibility is assessed, called flexibility assessment period. Based on s_t and z_t , we design the following logic:

- $s_t = 1$ and $z_t = 0$: time instant t is within the flexibility period, and hence $u_t = 0$.
- $s_t = 0$ and $z_t = 0$: time instant t is before the flexibility period, and $u_t \in \mathbb{B}$.
- $s_t = 0$ and $z_t = 1$: time instant t is after flexibility period, and $u_t \in \mathbb{B}$.

The above logic can be mathematically formulated as the following linear constraints:

$$u_t \leq 1 - s_t, \quad (7a)$$

$$s_{t+1} \geq s_t - z_{t+1}, \quad (7b)$$

$$s_t + z_t \leq 1, \quad (7c)$$

$$z_{t+1} \geq z_t. \quad (7d)$$

In Fig. 4, a schematic illustration of the above logics is provided, where the flexibility assessment period is defined by \mathcal{T} , and the flexibility period is defined by \mathcal{F} , whose formal definition is given below.

$$\mathcal{F} := \{t | s_t = 1, t \in \mathcal{T}\} \subseteq \mathcal{T}. \quad (8)$$

The flexibility period \mathcal{F} gives the optimal flexibility capacity, i.e., the time period within \mathcal{T} that the HP can be off without violating system constraints, that the BMS will promise to the grid operator.

Finally, flexibility assessment can be mathematically formulated as the following optimization problem

$$\min_{u_t, s_k, z_k} J_o - J_f \quad (9a)$$

$$\text{s.t. } x_{t+1} = f(x_t, u_t, d_t), \quad (9b)$$

$$x_t \text{ satisfy (5), } u_t \text{ satisfy (6),} \quad (9c)$$

$$\forall t = 0, 1, 2, \dots, N-1, \quad (9d)$$

$$(u_k, s_k, z_k) \text{ satisfy (7), } \forall k \in \mathcal{T} \quad (9e)$$

where N is the length of prediction horizon, $J_o = \sum_{t=1}^N l_t(x_t, u_{t-1})$ is the total operational cost of the HPTES

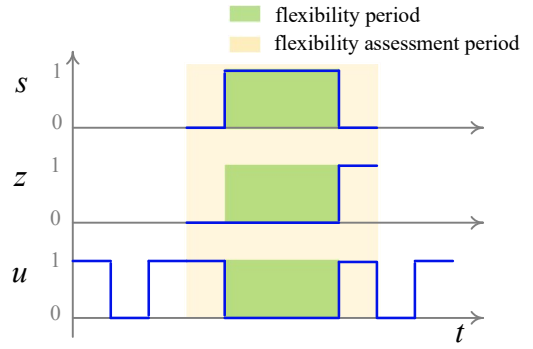


Fig. 4: Schematic of the logic in (7) indicating flexibility periods.

system within the prediction horizon with $l_t(x_t, u_{t-1})$ as the t -th stage cost, $J_f = \lambda \sum_{t \in \mathcal{T}} s_t$ is the revenue of flexibility that is proportional to the length of flexibility period, $\lambda \in \mathbb{R}_+$ is a scaling factor, $f(x_t, u_t, d_t)$ is the control-oriented model of the HPTES system introduced in (2) and (4) with system states x_t as the temperature vector of different water layers and pipelines, d_t as the mass flow rate of hot water consumption \dot{m}_s at time instant t , and u_t the binary control input of HP. For the sake of brevity, the detailed expressions of $f(x_t, u_t, d_t)$ are given in Section VI.

Remark 2: The optimization problem (9) aims at optimally balancing the operational cost and the benefit of promising a certain capacity for flexibility as DSM to the power grid. If the operational cost term J_o in the objective function is omitted, solving (9) will allow us to calculate the maximal capacity of energy flexibility. Namely, the longest consecutive time period during which the HP can remain off without violating system constraints. It should be noted that, compared with a typical economic MPC problem formulation, the proposed flexibility assessment problem only entails introducing extra linear constraints (7), and is independent of the structure of the system dynamics (9b). These properties are beneficial to the scalability and applicability of the proposed scheme.

B. Flexibility Exploitation

After solving the optimization problem (9), BMS will send the promised flexibility capacity \mathcal{F} to the power grid. Based on this information, the grid operator will subsequently generate a feasible DR request $\mathcal{R} = \{t | t \in \mathcal{F}\} \subseteq \mathcal{F}$ to specify the exact time instants that the HP is required to be off. Namely,

$$u_t = 0, \forall t \in \mathcal{R}. \quad (10)$$

For achieving this DR request, in BMS a general MPC problem can be formulated by imposing the constraints (10). An example for such a formulation will be shown in (14) of Section IV. Since the DR request \mathcal{R} is feasible w.r.t. the flexibility capacity \mathcal{F} , i.e., $\mathcal{R} \subseteq \mathcal{F}$, it can be guaranteed that the DR request in (10) can be achieved without violating system constraints owing to the fact that $u_t = 0$ ($\forall t \in \mathcal{F}$) is always a feasible solution.

IV. SIMULATION RESULTS

In order to demonstrate the effectiveness of the proposed scheme, a numerical simulation is performed for an HPTES system, which is based on a real installation for providing domestic hot water in an office building in the Netherlands, see Fig. 5. This system is composed of one air-to-water HP and two 500L water tanks. The hot water is used for dish washing in dining hall and showering in fitness rooms in the building. The detailed model and corresponding parameters of this HPTES system are provided in Section VI.



(a) Air-to-water HP.



(b) Two 500L water tanks.

Fig. 5: Motivating example of an HPTES system for our numerical case-study.

In our case study, the HP is operated during working hours 7:00 am - 5:30 pm. To implement the proposed strategy, hot water consumption d_t and its predicted value \hat{d}_t are needed. Fig. 6 gives the real hot water consumption profile, which is used for simulating the dynamics of the HPTES system, and the predicted value, which is used for MPC design. The non-negligible prediction errors visible in the figure allow for testing the robustness of our proposed scheme.

To provide qualified hot water, the temperature of the water supplied to buildings, in our case the water temperature at the top of Tank 1 that is denoted as T_1 , has to satisfy

$$55 \leq T_1 \leq 75. \quad (11)$$

In addition, to mitigate the risk of legionella bacteria, which proliferate between 20°C - 50°C, and to provide hot water with sufficient temperature, it is recommended to maintain T_1 above 60°C most of the time:

$$T_1 \geq 60, \text{ for most of the time.} \quad (12)$$

Since both constraints (11) and (12) are hard constraints, to ensure the feasibility of the proposed MPC design, they are relaxed as soft constraints:

$$55 - \delta_1 \leq T_1 \leq 75 + \delta_1, \quad (13a)$$

$$T_1 \geq 60 - \delta_2, \quad (13b)$$

where $\delta_1 > 0$ and $\delta_2 > 0$ are slack variables that will be penalized in the MPC objection function, see (14).

During the whole simulation period, the flexibility task is performed every 3 hours (3 times in total). For flexibility assessment in (9), the prediction horizon is selected as 4 hours, and the first 3 hours are chosen as flexibility assessment period. The boundaries of flexibility assessment periods are indicated with red dash lines in Fig. 8. The objective function of the flexibility assessment (9) is chosen

as $-\sum_{t \in \mathcal{T}} s_t$, which implies computing the longest period during which HP can remain off without violating system constraints.

After finishing the flexibility assessment task, the corresponding DR request is set as $\mathcal{R} = \mathcal{F}$. Namely, the power grid tries to utilize all available energy flexibility to reduce electricity consumption during the flexibility period. For achieving the DR request, the following economic MPC formulation is adopted:

$$\min_{u_t, \delta} \sum_{t=0}^N e_t u_t + M_1 \delta_1 + M_2 \delta_2 \quad (14a)$$

$$\text{s.t. } x_{t+1} = f(x_t, u_t, \hat{d}_t), \quad (14b)$$

$$x_t \text{ satisfy (13), } u_t \text{ satisfy (6),} \quad (14c)$$

$$\forall t = 0, 1, 2, \dots, N-1 \quad (14d)$$

$$u_k = 0, \forall k \in \mathcal{R}, \quad (14e)$$

where e_t represents the electricity price at time instant t , δ_1 and δ_2 are the slack variables for relaxing the input and state constraints (13) if needed, M_1 and M_2 are corresponding penalties. A typical electricity price in the Netherlands during the simulation period is shown in Fig. 7, which is used in our simulation.

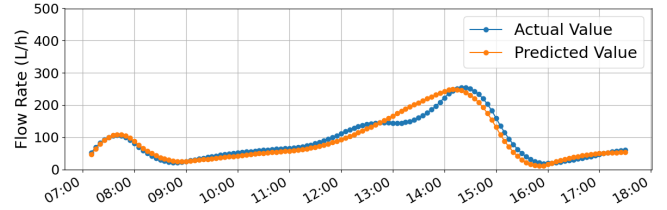


Fig. 6: Hot water consumption and its prediction.

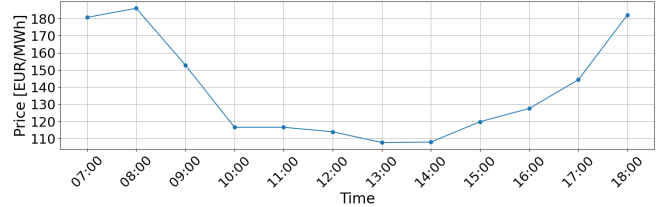


Fig. 7: Electricity price used in simulation.

Simulation results are given in Fig. 8 - 9. Fig. 8 depicts the HP input signals during the simulation period. It can be seen that during all flexibility periods, which are green shaded regions, the HP is kept off to reduce its energy consumption for providing DR services. Fig. 9 shows the water temperature at the top of Tank 1. It is clear that during the whole simulation period, our proposed approach is able to maintain the temperature within permissible range, which is crucial for providing qualified hot water for buildings. Table I compares the operational performance of the proposed MPC approach with that of the existing rule-based approach implemented for the HPTES installation. With the rule-based approach, the HP is operated only based on the temperature

	Rule-Based Approach	MPC
Average Water Temperature (°C)	65.53	64.85
Maximal Constraint violation (°C)	4.43	4.12
Energy Consumption(kWh)	64.17 (100%)	62.50 (97.40%)
Energy Cost (Euro)	8.69 (100%)	8.41 (96.78%)

TABLE I: Operational performance of the MPC and the rule-based scheme.

of the water tanks: if water temperature at the bottom of Tank 2 is higher than 62°C, HP is off; if temperature at the top of Tank 1 is lower than 62°C, HP is on. Clearly, the proposed MPC approach gives better operational performance than the existing rule-based approach even under the presence of flexibility exploitation, which usually degrades the economical performance of MPC. In summary, the proposed MPC approach is not only able to provide DR services by exploiting the energy flexibility of the HPTES system, but is also capable of operating the HPTES system safely and efficiently to provide qualified domestic hot water usage.

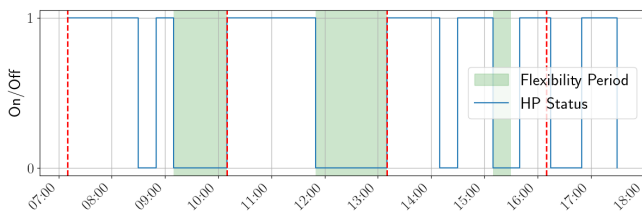


Fig. 8: Control input signals of heat pump.

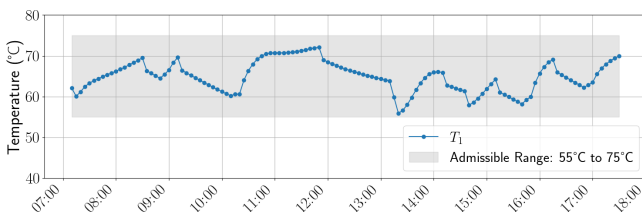


Fig. 9: Water temperature at the top of Tank 1.

V. CONCLUSIONS

This paper proposed an energy flexible MPC scheme for assessing and exploiting the energy flexibility of HPTES systems to provide demand response services. With the proposed approach, the energy flexibility potential of the HPTES system is quantitatively analyzed by solving a typical mixed-integer economic MPC problem with extra linear constraints. Then the flexibility is activated via feasible DR requests to achieve the reduction of energy consumption without violating system constraints. The proposed scheme provides a systematical approach to take advantage of the flexibility potential of HPTES systems to achieve demand-side management. The efficacy of our design is demonstrated via the simulation results based on a real-world HPTES installation. Future work includes implementing pilot experiments of the proposed scheme on the real-world HPTES installation.

REFERENCES

- [1] D. Government, “Klimaatnota 2022,” 2022. [Online]. Available: <https://www.rijksoverheid.nl/documenten/publicaties/2022/11/01/klimaatnota-2022>
- [2] F. Bübbing, J. Warrington, P. Heer, R. S. Smith, and J. Lygeros, “Robust MPC with data-driven demand forecasting for frequency regulation with heat pumps,” *Control Engineering Practice*, vol. 122, p. 105101, 2022.
- [3] European Commission, Directorate General for Energy, “Clean energy for all europeans package,” 2019. [Online]. Available: https://energy.ec.europa.eu/topics/energy-strategy/clean-energy-all-europeans-package_en
- [4] E. Commission, “Heat pumps are key to enabling the clean energy transition and achieving the EU’s carbon neutrality goal by 2050,” 2022. [Online]. Available: https://energy.ec.europa.eu/topics/energy-efficiency/heat-pumps_en
- [5] C. Ermel, M. V. Bianchi, A. P. Cardoso, and P. S. Schneider, “Thermal storage integrated into air-source heat pumps to leverage building electrification: A systematic literature review,” *Applied Thermal Engineering*, p. 118975, 2022.
- [6] B. Alimohammadisagvand, J. Jokisalo, S. Kilpeläinen, M. Ali, and K. Sirén, “Cost-optimal thermal energy storage system for a residential building with heat pump heating and demand response control,” *Applied Energy*, vol. 174, pp. 275–287, 2016.
- [7] R. Tang and S. Wang, “Model predictive control for thermal energy storage and thermal comfort optimization of building demand response in smart grids,” *Applied Energy*, vol. 242, pp. 873–882, 2019.
- [8] K. J. Kircher and K. M. Zhang, “Model predictive control of thermal storage for demand response,” in *2015 American Control Conference (ACC)*. IEEE, 2015, pp. 956–961.
- [9] R. Renaldi, A. Kiprakis, and D. Friedrich, “An optimisation framework for thermal energy storage integration in a residential heat pump heating system,” *Applied energy*, vol. 186, pp. 520–529, 2017.
- [10] F. D’Ettore, M. De Rosa, P. Conti, D. Testi, and D. Finn, “Mapping the energy flexibility potential of single buildings equipped with optimally-controlled heat pump, gas boilers and thermal storage,” *Sustainable Cities and Society*, vol. 50, p. 101689, 2019.
- [11] H. Golmohamadi, K. G. Larsen, P. G. Jensen, and I. R. Hasrat, “Integration of flexibility potentials of district heating systems into electricity markets: A review,” *Renewable and Sustainable Energy Reviews*, vol. 159, p. 112200, 2022.
- [12] Y. Li, N. Yorke-Smith, and T. Keviczky, “Unlocking energy flexibility from thermal inertia of buildings: A robust optimization approach,” in *2023 62nd IEEE Conference on Decision and Control (CDC)*. IEEE, 2023, pp. 2555–2562.
- [13] M. Kongsman, E. Werkman, and in collaboration with TC 205 WG 18 members, “S2 white paper,” 2023. [Online]. Available: <https://s2standard.org/>
- [14] S. Rastegarpour, M. Ghaemi, and L. Ferrarini, “A predictive control strategy for energy management in buildings with radiant floors and thermal storage,” in *2018 SICE International Symposium on Control Systems (SICE ISCS)*. IEEE, 2018, pp. 67–73.
- [15] R. G. Junker, A. G. Azar, R. A. Lopes, K. B. Lindberg, G. Reynders, R. Relan, and H. Madsen, “Characterizing the energy flexibility of buildings and districts,” *Applied Energy*, vol. 225, pp. 175–182, 2018.
- [16] S. Ø. Jensen, A. Marszał-Pomianowska, R. Lollini, W. Pasut, A. Knotzer, P. Engelmann, A. Stafford, and G. Reynders, “Tea ebc annex 67 energy flexible buildings,” *Energy and Buildings*, vol. 155, pp. 25–34, 2017.

VI. APPENDIX

In the following, the detailed model and parameters of the HPTES used in our simulation are provided. For the stratified tank model, Tank 1 and Tank 2 are modeled with 2 and 4 layers, respectively. The thermal dynamics is given in (15), the definition of the state variables is given in Table II, and the value of the parameters in (15) is in Table III.

$$x_{k+1}^1 = u_k \left(x_{k+1}^2 + \frac{Q_{hp}}{m_p c_p} \right) + (1 - u_k) \left(x_k^1 - \frac{\Delta t}{m_{pipe} c_p} (R_{pipe} (x_k^1 - T_k^{amb}) + R_{pipe,upper} (x_k^1 - x_k^3) + R_{pipe,bottom} (x_k^1 - x_k^8)) \right), \quad (15a)$$

$$x_{k+1}^2 = T_s \frac{\dot{m}_s}{\dot{m}_p} + x_k^8 \left(1 - \frac{\dot{m}_s}{\dot{m}_p} \right), \quad (15b)$$

$$x_{k+1}^3 = x_k^3 + \frac{\Delta t}{m_1 c_p} \left(\dot{m}_p c_p (x_k^1 - x_k^3) u_k - (\dot{m}_c - \dot{m}_s) c_p \Delta T_c - R_{12} (x_k^3 - x_k^4) + \dot{m}_s c_p (x_k^4 - x_k^3) (1 - u_k) \right) + \Delta T_{off} \cdot (u_k - u_{k-1}) \cdot u_{k-1}, \quad (15c)$$

$$x_{k+1}^4 = x_k^4 + \frac{\Delta t}{m_2 c_p} \left((\dot{m}_p - \dot{m}_s) c_p (x_k^3 - x_k^4) u_k + R_{12} (x_k^3 - x_k^4) - R_{23} (x_k^4 - x_k^5) + \dot{m}_s c_p (x_k^5 - x_k^4) (1 - u_k) \right), \quad (15d)$$

$$x_{k+1}^5 = x_k^7 + \frac{\Delta t}{m_3 c_p} \left((\dot{m}_p - \dot{m}_s) c_p (x_k^4 - x_k^5) u_k + R_{23} (x_k^4 - x_k^5) - R_{34} (x_k^5 - x_k^6) + \dot{m}_s c_p (x_k^6 - x_k^5) (1 - u_k) \right), \quad (15e)$$

$$x_{k+1}^6 = x_k^8 + \frac{\Delta t}{m_4 c_p} \left((\dot{m}_p - \dot{m}_s) c_p (x_k^5 - x_k^6) u_k + R_{34} (x_k^5 - x_k^6) - R_{45} (x_k^6 - x_k^7) + \dot{m}_s c_p (x_k^7 - x_k^6) (1 - u_k) \right), \quad (15f)$$

$$x_{k+1}^7 = x_k^7 + \frac{\Delta t}{m_5 c_p} \left((\dot{m}_p - \dot{m}_s) c_p (x_k^6 - x_k^7) u_k + R_{45} (x_k^6 - x_k^7) - R_{56} (x_k^7 - x_k^8) + \dot{m}_s c_p (x_k^8 - x_k^7) (1 - u_k) \right), \quad (15g)$$

$$x_{k+1}^8 = x_k^8 + \frac{\Delta t}{m_6 c_p} \left((\dot{m}_p - \dot{m}_s) c_p (x_k^7 - x_k^8) u_k + R_{56} (x_k^7 - x_k^8) + \dot{m}_s c_p (T_s - x_k^8) (1 - u_k) \right), \quad (15h)$$

$$Q_{hp} = \text{COP} \cdot P_r \cdot u, \quad (15i)$$

$$\text{COP} = a_1 + a_2 T_{in, hp} + a_3 T_{amb} + a_4 T_{in, hp} T_{amb}, \quad (15j)$$

$$T_{in, hp} = \Delta T_{he} + T_{out, tank}. \quad (15k)$$

In (15), the thermal loss $\dot{Q}_{wall, j}$ in (4) is omitted since the HPTES system is well-insulated such that the thermal loss is negligible. Equality (15k) is derived via

$$T_{out, hp} - T_{in, hp} = T_{in, tank} - T_{out, tank} \quad (16)$$

with $\Delta T_{he} := T_{out, hp} - T_{in, tank}$ as a relatively stable temperature difference, which is true when the heat exchanger is operated with high efficiency.

In addition, the term $\Delta T_{off} \cdot (u_k - u_{k-1}) \cdot u_{k-1}$ in (15c) is used to reflect a special phenomenon of the temperature drop ΔT_{off} for water in the top of Tank 1 when HP is switched from on to off, which is caused by the HP and the circulation pump of water tanks being out of sync in our HPTES system.

State	Description	Units
x^1	The inlet water temperature of the water tanks, $T_{in, tank}$	$^{\circ}\text{C}$
x^2	The outlet water temperature of the water tanks $T_{out, tank}$	$^{\circ}\text{C}$
x^3	The temperature of the 1st layer of the water tanks T_1	$^{\circ}\text{C}$
x^4	The temperature of the 2nd layer of the water tanks T_2	$^{\circ}\text{C}$
x^5	The temperature of the 3rd layer of the water tanks T_3	$^{\circ}\text{C}$
x^6	The temperature of the 4th layer of the water tanks T_4	$^{\circ}\text{C}$
x^7	The temperature of the 5th layer of the water tanks T_5	$^{\circ}\text{C}$
x^8	The temperature of the 6th layer of the water tanks T_6	$^{\circ}\text{C}$

TABLE II: Description of notations in (15).

Term	Description	Value	Units
Δt	sampling time	1/3	h
c_p	Specific heat capacity of water	4186	J/kg · K
R_{pipe}	Thermal resistance for outlet pipe of the heat exchanger	0.30	W/K
$R_{pipe,upper}$	Thermal resistance between outlet pipes of the heat exchanger and the upper layer of Tank 1	0	W/K
$R_{pipe,bottom}$	Thermal resistance between outlet pipes of the heat exchanger and the bottom layer of Tank 2	2	W/K
R_{12}	Thermal resistance between the 1st and 2nd layers of the water tanks	0.24	W/K
R_{23}	Thermal resistance between the 2nd and 3rd layers of the water tanks	0.24	W/K
R_{34}	Thermal resistance between the 3rd and 4th layers of the water tanks	0.49	W/K
R_{45}	Thermal resistance between the 4th and 5th layers of the water tanks	0.54	W/K
R_{56}	Thermal resistance between the 5th and 6th layers of the water tanks	0.53	W/K
m_{pipe}	Mass of the outlet pipe of the heat exchanger	3.27	kg
m_1	Mass of the 1st layers of the water tanks	250	kg
m_2	Mass of the 2nd layers of the water tanks	250	kg
m_3	Mass of the 3rd layers of the water tanks	169.66	kg
m_4	Mass of the 4th layers of the water tanks	95.38	kg
m_5	Mass of the 5th layers of the water tanks	136.67	kg
m_6	Mass of the 6th layers of the water tanks	98.29	kg
ΔT_{he}	Temperature difference of the heat exchanger	2.84	$^{\circ}\text{C}$
ΔT_c	Temperature difference in the demand pipe	1.76	$^{\circ}\text{C}$
T_s	Temperature of the water in supply pipe	13	$^{\circ}\text{C}$
ΔT_{off}	Temperature drop of the heat pump's deactivation	2.5	$^{\circ}\text{C}$
T_{amb}	Ambient Temperature	18.5	$^{\circ}\text{C}$
\dot{m}_s	Flow rate in the supplement pipe	-	kg/h
\dot{m}_c	Flow rate in the demand circulation pipe	1100	kg/h
\dot{m}_p	Flow rate in the main circulation pipe	880	kg/h
a_1	Parameter in COP	3.3297	-
a_2	Parameter in COP	-0.0423	-
a_3	Parameter in COP	0.0219	-
a_4	Parameter in COP	0.0003	-

TABLE III: Nominal values of the parameters in (15).